

# Density Functional Study on the Structures and Energies of the $\text{Ti}_2\text{C}_2$ Cluster

R. Sumathi and M. Hendrickx\*

Department of Chemistry, University of Leuven, Celestijnenlaan 200F, B-3001 Leuven, Belgium

Received: June 25, 1998

The structures and energies of the binary dititanium dicarbide,  $\text{Ti}_2\text{C}_2$ , in the lowest singlet, triplet, and quintet states have been investigated by density functional theory using the hybrid B3LYP functionals. Geometries and frequencies for a number of isomeric structures are presented at the B3LYP level. A rhombic structure with a transannular C–C bond (**VI**) is found to be the global  $\text{Ti}_2\text{C}_2$  minimum. The other four-membered planar ring structures (**VII** and **VIII**) derived from the two-fold addition of carbon to the Ti–Ti or the Ti–C bond of the cyclic ( $C_{2v}$ )  $\text{Ti}_2\text{C}$  are characterized as higher energy local minima. A linear structure (**I**) with terminal titanium atoms is found to be a higher energy minimum in its singlet, triplet, and quintet potential energy surfaces (PES) and has a bonding characteristic of a cumulene-like valence structure. Besides, a unique nonplanar  $C_{2v}$  structure, which has not been obtained in the isovalence electronic  $\text{Si}_2\text{C}_2$  and  $\text{SiC}_3$  systems, has been identified as a minimum. Cyclic structures are energetically favored over the linear structures. A comparison with the tetra-atomic group IVA silicon–carbon clusters is given, where appropriate.

## 1. Introduction

Especially stable metal–carbon clusters having the stoichiometry  $\text{M}_8\text{C}_{12}$  have recently been reported by Castleman and co-workers for the metals titanium, vanadium, hafnium, niobium, and zirconium,<sup>1–14</sup> as well as for several metal mixtures.<sup>13</sup> Duncan and co-workers<sup>15</sup> have reported metal–carbon clusters of the same special 8/12 stoichiometry in mass distributions of iron, chromium, and molybdenum. Castleman and co-workers have proposed a pentagonal dodecahedron structure with  $T_h$  symmetry for the  $\text{M}_8\text{C}_{12}$  cluster, which is consistent with the results of saturation chemisorption studies<sup>5</sup> and ion chromatography experiments.<sup>16</sup> However, theoretical calculations indicate that other structures ( $T_d$  or  $D_{2d}$  symmetry) slightly distorted from the  $T_h$  cage are more likely,<sup>17–31</sup> and these structures are also supported by chemisorption experiments.<sup>32</sup> In spite of the intensive research on the metcars, the structure and bonding of these unique clusters are still not well understood. A systematic and thorough experimental and theoretical investigation on the detailed structure and bonding of the small titanium carbide clusters,  $\text{Ti}_n\text{C}_m$  may provide this information and may lead to valuable insight into the growth and formation of metcars. In line with this perspective, Wang et al.<sup>33</sup> studied the vibrationally resolved photoelectron spectral study of  $\text{TiC}_x$  ( $x = 2–5$ ) clusters and reported their adiabatic affinities and ground state vibrational frequencies. Our studies on  $\text{TiC}_x$  ( $x = 2–4$ ) at CASSCF,<sup>34,35</sup> MRCI,<sup>34</sup> and DFT<sup>34,35</sup> levels established their ground state geometry to be a ring-type structure with the coordination of titanium to all the carbons of the cluster. The  $\text{C}_x$  moiety bents slightly away from its most favorable linear configuration and leads to stable strained rings via Ti–C bonds. These clusters indeed represent systems containing a higher proportion of carbon to metal as compared to the bulk TiC fcc phase (M:C = 1:1) or the metcars (M:C = 1:1.5). The bulk TiC phase is marked by strong covalent (partially ionic) bonds between the transition metal and carbon atoms; there is practically no bonding between either transition metals or carbon atoms, and therefore this phase is stabilized by TiC bonds. On the other hand, our investigations<sup>36</sup> on the  $\text{Ti}_2\text{C}_3$  cluster, a prototypical

cluster with the same composition as in the metcars, revealed a planar pentagonal ring structure with a  $\text{C}_2$  base that was found to be stabilized by  $\text{C}_2^-$  bonding involving charge transfer from Ti to C. Hence, in order to establish whether the existence of undissociated  $\text{C}_2$  units is unique of the metal clusters having a composition of metcars, we have investigated the  $\text{Ti}_2\text{C}_2$  cluster whose metal to carbon composition is the same as that of the bulk TiC. The present paper will therefore, deal with the lowest-energy structures of the various  $\text{Ti}_2\text{C}_2$  isomers, and where appropriate, comparison will be given with the analogous well-studied group IVA clusters ( $\text{C}_4$ ,  $\text{Si}_4$ ,  $\text{SiC}_3$ ,  $\text{Si}_2\text{C}_2$ ,  $\text{Si}_3\text{C}$ ), which possess the same number of valence electrons as in  $\text{Ti}_2\text{C}_2$ . Such a comparison is worthwhile to identify the impact of the fundamental differences between  $s^2p^2$  and  $s^2d^2$  configurations. The tetra-atomic 16-valence-electron  $\text{C}_4$  shows a slight preference for the rhombic over linear structure.<sup>37</sup> The linear structure for  $\text{C}_4$  has been detected in the infrared,<sup>38</sup> while the corresponding cyclic structure has always eluded detection. Nevertheless, Coulomb explosion<sup>39</sup> and electron photodetachment<sup>40</sup> experiments definitely suggest the existence of a rhombic  $\text{C}_4$  isomer. Martin et al.<sup>41</sup> in their ab initio work on the vibrational spectra of carbon clusters, suggested that an unassigned absorption at  $1284\text{ cm}^{-1}$  belongs to cyclic  $\text{C}_4$ . On the whole, for  $\text{C}_4$  clusters linear and monocyclic singlet ring structures are competitive. In contrast, the related 16e  $\text{Si}_4$  strongly favors a rhombic form.<sup>42</sup> The tetra-atomic mixed carbon–silicon clusters  $\text{SiC}_3$  and  $\text{Si}_2\text{C}_2$  have been shown theoretically<sup>43,44</sup> to have a rhombic minimum incorporating a transannular C–C bond. The only work, to our knowledge, on  $\text{Ti}_2\text{C}_2$  corresponds to the density functional study of Reddy and Khanna<sup>45</sup> using the local density approximations (LDA). They employed pseudopotentials to replace the deep cores and their basis set consists of 5s, 2p, and 4d Gaussians for Ti and 5s and 4p Gaussians for C. Indeed, in this study, Reddy and Khanna optimized the geometry by assuming a  $\text{C}_2$  and  $\text{Ti}_2$  moiety perpendicular to each other and by varying the C–C and Ti–Ti distances and the separation between their centers to minimize the energy. They found a nearly square configuration ground state with no bonding between the C atoms

as in bulk TiC. However, relevant to this study, no other structures were reported by the authors. Furthermore, it is worthwhile to mention that the metcar formation occurs at plasma temperature and, consequently, it could involve higher energy isomers of  $\text{Ti}_2\text{C}_2$  as intermediates in cluster growth besides the thermochemically most stable global minimum. As a first step toward understanding, it is therefore essential to identify and characterize the different isomers of  $\text{Ti}_2\text{C}_2$ . Hence, the objective of the present study is to provide a comprehensive and detailed survey of the potential energy hypersurface of the binary  $\text{Ti}_2\text{C}_2$  cluster.

## 2. Computational Details

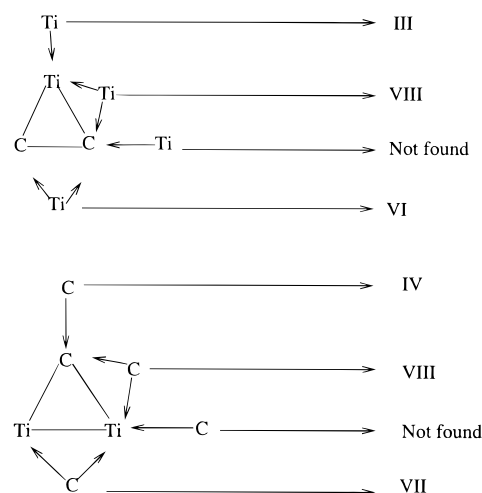
The DFT method was employed for determining the various stationary points on the multidimensional  $\text{Ti}_2\text{C}_2$  potential energy surface. The exchange functional in the hybrid B3LYP method<sup>46</sup> is composed of three terms, including the Hartree–Fock exchange functional. The correlation functional is that of Lee, Yang, and Parr.<sup>47</sup> MULLIKEN<sup>48</sup> has been used for the B3LYP optimizations. It is worthwhile to mention that the implementation of B3LYP in the commonly used quantum chemical packages like GAUSSIAN94,<sup>49</sup> TURBOMOLE,<sup>50</sup> and MULLIKEN is different. Hertwig and Koch<sup>51</sup> have traced this discrepancy between the former two packages to the two different formulations of the VWN local correlation functional. They have also shown that the differences are rather small for structural parameters and zero point energies. In the program MULLIKEN, a slightly modified version of the B3LYP functional is implemented wherein the local correlation functional of VWN<sup>52</sup> is replaced by the functional from Perdew et al.<sup>53</sup> Except for the GAUSSIAN, the other two packages allow only for the numerical estimation of force constants and thereby frequencies. Hence, in our study, various initial structures were chosen and a complete geometry optimization within a given symmetry group was then carried out in their singlet, triplet, and quintet multiplicities using the quantum chemical package MULLIKEN until a structure corresponding to a stationary point was found. All such stationary points were further reoptimized and tested with respect to their character by a vibrational analysis checking for possible imaginary frequencies using the GAUSSIAN94 series of program. We present here the energies and frequencies as obtained from the GAUSSIAN94 program. Altogether a total of nine stationary points have been studied.

The titanium basis set was a (14s,11p,6d,3f/8s,6p,4d,1f) formed from Wachter's<sup>54</sup> (14s,9p,5d) basis set with the addition of Hay's<sup>55</sup> diffuse 3d function. The f Slater type function (STF) exponent was taken from Bauschlicher et al.<sup>56</sup> and the Gaussian type function (GTF) exponents were derived by using Stewart's contraction fits.<sup>57</sup> For carbon, the standard DZP (9s,5p,1d/4s,2p,1d) basis set was used. The favored geometries at the B3LYP level for  $\text{Ti}_2\text{C}_2$  have then been examined at the multiconfiguration level CASSCF (14 electrons in 13 orbitals) with the sole purpose to understand the orbital picture. However, no attempt has been made to either optimize the geometry at the CASSCF level or to estimate the single point energies of the various structures, since a full valence space calculation corresponds to 16 electrons and 20 orbitals, which is beyond our resources. MOLPRO-96<sup>58</sup> has been employed for CASSCF calculations.

## 3. Results and Discussion

The ground state of dititanium dicarbide can be formed from the addition of two TiC molecules or by the addition of C to  $\text{Ti}_2\text{C}$  or by the addition of Ti to  $\text{TiC}_2$ . The ground state of

### SCHEME 1



titanium ( $3d^24s^2$ ) and carbon ( $2s^22p^2$ ) corresponds respectively to the  $^3F$  and  $^3P$  state. The calculations<sup>59</sup> confirm that the ground state of TiC is the  $^3\Sigma^+$  state. Our calculations<sup>34</sup> on  $\text{TiC}_2$  and  $\text{Ti}_2\text{C}$  establish a triplet ground state with a cyclic  $C_{2v}$  structure. Hence the resultant  $\text{Ti}_2\text{C}_2$  could have any of the multiplicities ranging from a singlet to a quintet. Hence, geometry optimizations have been performed for the various electronic states at the B3LYP level, starting from different nuclear arrangements that included linear (**I**, **II**), planar three-membered cyclic (**III**, **IV**), planar four-membered cyclic (**V**, **VI**, **VII**, **VIII**), and nonplanar tetrahedral (**IX**) geometries.

Being isovalent with  $\text{TiC}_3$ , which is found to have a ring structure ("fan"), and containing a  $C_3$  submolecule with double bonds, it is likely furthermore that the ground state could be a strained ring. Also  $\text{Ti}_2\text{C}_2$  could be visualized as the addition product of Ti to  $\text{TiC}_2$ , which is predicted<sup>34</sup> to have a cyclic  $C_{2v}$  structure with tangling bonds on titanium (see Scheme 1) as the ground state geometry. The 2-fold addition of Ti to either one of the Ti–C bonds or the C–C bond of the cyclic  $\text{TiC}_2$  cluster leads to the planar four-membered rhomboidal (**VIII**) and rhombic (**VI**) isomers (with a transannular C–C bond). Similar 2-fold addition of C to the Ti–Ti or the Ti–C bond of the cyclic  $\text{Ti}_2\text{C}$  cluster results in rhombic (**VII**) (with a transannular Ti–Ti bond) and rhomboidal (**VIII**) isomers. Besides,  $\text{Ti}_2\text{C}_2$  could also result from the 1-fold addition of either atomic carbon to  $\text{Ti}_2\text{C}$  (**IV**) or of titanium to  $\text{TiC}_2$  (**III**) (see Scheme 1). In addition to these planar cyclic isomers, a nonplanar tetrahedral isomer, viz., **IX**, has also been considered for geometry optimizations.

The equilibrium geometries obtained for the  $\text{Ti}_2\text{C}_2$  isomers are given in Figures 1 and 2. Bond lengths are given in angstroms and bond angles in degrees. The numbers inside the parentheses and square parentheses correspond respectively to the singlet and quintet state geometries. Most of these isomers have geometries that allow for multiple carbon–carbon bonding, and we expect them to be energetically favored due to the relative strength of C–C bonds as compared to the Ti–C and Ti–Ti bonds. Tables 1 and 2 give the harmonic vibrational frequencies for the isomers of  $\text{Ti}_2\text{C}_2$ . The absolute energy of all the structures in various electronic states of  $\text{Ti}_2\text{C}_2$  is also tabulated in Tables 1 and 2 along with the expectation value for the  $\langle S^2 \rangle$  operator, which gives a measure of the extent of spin contamination. The relative energy of the various isomers is shown in Figure 3.

The unique nonplanar structure **IX** has been optimized using different functionals and basis sets in order to test its stability.

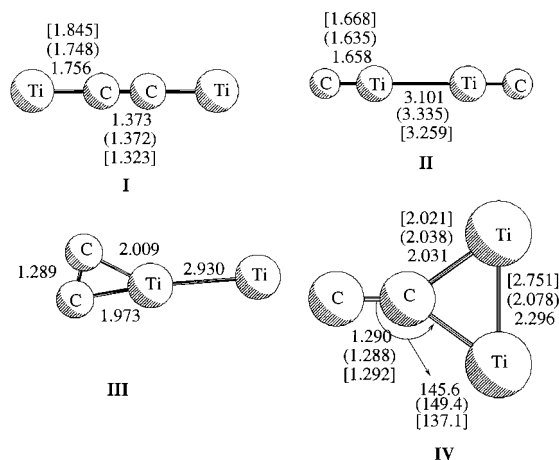


**Figure 1.** Optimized geometries for the singlet, triplet, and quintet isomers of the linear and three-membered ring isomers of  $\text{Ti}_2\text{C}_2$  at the B3LYP level of theory.

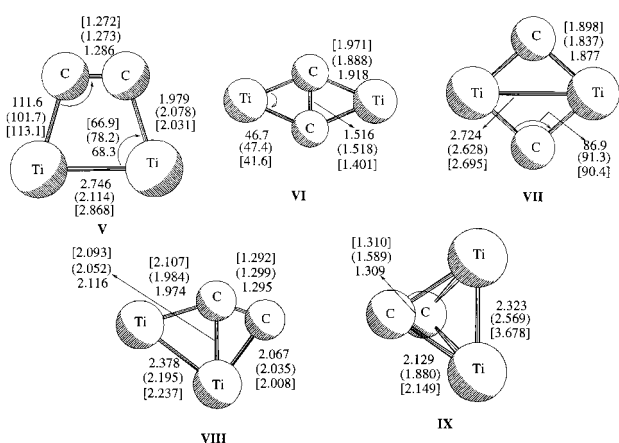


**Figure 2.** Optimized geometries for the singlet, triplet, and quintet isomers of the ring structures of  $\text{Ti}_2\text{C}_2$  at the B3LYP level of theory.

The optimized geometrical parameters obtained by the various methods are tabulated in Table 3. The binding energy of the cluster with respect to various dissociation limits viz.,  $2\text{Ti} + 2\text{C}$ ,  $\text{Ti}_2 + \text{C}_2$ ,  $\text{Ti}_2\text{C} + \text{C}$ , and  $\text{TiC}_2 + \text{C}$  is given in Table 4.

**3.1. Linear Structures.** The lowest energy linear isomer of  $\text{Ti}_2\text{C}_2$  corresponds to the nuclear arrangement containing two terminal titanium atoms. The quintet electronic configuration, **Iq**, is favored over the triplet, which in turn is favored over the singlet via Hund's rules, and it displays strong C—C and Ti—C bonding, as expected for a cumulene-like valence structure in which the titaniums participate in multiple bonding. The C—C bond length (1.323 Å) is intermediate between that of a normal C—C double bond (1.337 Å in ethylene) and a normal triple bond (1.204 Å in acetylene). The C—C bond length is found to be larger than the ones found in  $\text{C}_4$  (1.288, 1.300 Å) by Bernholdt et al.<sup>60</sup> and the C—C bond lengths as found<sup>43</sup> for  $\text{SiC}_3$  (1.298, 1.307 Å). The C—Ti bond length of 1.845 Å is typical of a Ti=C double bond. The geometry of the quintet structure differs much from that of the singlet and triplet with respect to the C—Ti bond length (0.103 and 0.109 Å, respectively). In contrast to  $\text{C}_4$  whose most stable ground state structure corresponds to this linear isomer, in  $\text{Ti}_2\text{C}_2$ , the cyclic isomer **VIq** is the most favored geometry (see Figure 3). The isomer **Iq** lies 58.5 kcal/mol above the cyclic structure, **VIq** and is a stable minimum in all three potential energy surfaces. In the case of triplet and quintet states the spin densities are located on the terminal titanium atoms. A natural population analysis has been performed in terms of localized electron-pair bonding

**TABLE 1: Absolute Energies in Hartrees, Frequencies in  $\text{cm}^{-1}$ , Zero Point Energy (ZPE) in kcal/mol, and the Expectation Value of the  $S^2$  Operator for the Various Isomers of the  $\text{Ti}_2\text{C}_2$  Cluster**

species	absolute energy (ZPE)	frequencies	$\langle S^2 \rangle$
<b>Is</b>	-1774.830281(5.096)	123.1, 123.1, 338.5, 338.5, 360.8, 885.6, 1395.2	0.0
<b>It</b>	-1774.855348(5.033)	106.9, 107.0, 332.6, 332.6, 357.2, 906.7, 1377.4	2.0
<b>Iq</b>	-1774.856934(4.821)	73.7, 78.9, 243.6, 293.9, 320.6, 799.4, 1562.2	6.05
<b>IIs</b>	-1774.703284(3.167)	135.8i, 135.8i, 93.6, 93.6, 116.7, 953.6, 957.7	0.0
<b>IIt</b>	-1774.735554(3.358)	63.0, 63.0, 84.0, 84.0, 140.9, 956.4, 958.1	2.0
<b>IIq</b>	-1774.683736(2.809)	116.7i, 116.7i, 72.7i, 72.7i, 87.1, 921.9, 956.4	6.001
<b>IIIIt</b>	-1774.867347(4.302)	43.7i, 51.4, 152.7, 465.6, 614.0, 1725.2	2.073
<b>IVs</b>	-1774.907573(4.689)	166.8i, 94.6, 382.8, 415.7, 543.6, 1843.7	0.0
<b>IVt</b>	-1774.882354(4.568)	147.5i, 256.9, 273.9, 382.8, 484.8, 1796.8	2.003
<b>IVq</b>	-1774.838949(4.450)	67.5i, 160.7, 178.1, 446.2, 611.6, 1716.2	6.012
<b>Vs</b>	-1774.904958(4.699)	464.7i, 160.6i, 416.4, 425.8, 590.2, 1855.2,	0.0
<b>Vt</b>	-1774.900786(4.226)	488.3i, 145.0i, 217.5, 514.8, 523.7, 1700.4	2.260
<b>Vq</b>	-1774.929076(4.389)	303.2i, 104.8i, 190.9, 514.2, 529.7, 1835.5	6.0

**TABLE 2: Absolute Energies in Hartrees, Frequencies in  $\text{cm}^{-1}$ , Zero Point Energy (ZPE) in kcal/mol, and the Expectation Value of the  $S^2$  Operator for the Various Isomers of the  $\text{Ti}_2\text{C}_2$  Cluster**

species	absolute energy (ZPE)	frequencies	$\langle S^2 \rangle$
<b>VIs</b>	-1774.936282(4.309)	157.1, 338.4, 360.0, 543.2, 696.2, 919.6,	0.0
<b>VIIt</b>	-1774.907427(4.327)	103.5, 342.1, 411.6, 581.6, 668.5, 919.1	2.0
<b>VIq</b>	-1774.950594(5.067)	138.2, 310.3, 360.1, 702.9, 784.7, 1248.5	6.01
<b>VIIIs</b>	-1774.936282(5.062)	193.2, 438.7, 461.9, 730.2, 832.0, 885.0	0.0
<b>VIIIt</b>	-1774.866647(4.521)	229.9i, 398.2, 521.7, 596.5, 817.3, 829.5	2.0
<b>VIIq</b>	-1774.857665(2.607)	276.9i, 528.9i, 892.3i, 360.1, 731.8, 731.8	6.01
<b>VIIIIs</b>	-1774.938794(5.578)	287.3, 321.5, 436.6, 528.7, 664.0, 1663.5	0.0
<b>VIIIIt</b>	-1774.936559(5.062)	161.7, 324.2, 403.9, 483.9, 533.7, 1633.1	2.016
<b>VIIIq</b>	-1774.913023(5.259)	191.9, 338.3, 383.5, 503.1, 572.1, 1689.7	6.002
<b>IXs</b>	-1774.914979(4.878)	256.6, 442.1, 485.1, 627.4, 697.7, 903.7	0.0
<b>IXt</b>	-1774.913757(4.276)	248.1i, 326.5i, 319.1, 333.5, 435.5, 1576.9	2.027
<b>IXq</b>	-1774.925983(4.577)	219.8, 304.1, 316.5, 318.4, 449.8, 1593.2	6.027
<b>TiC(<math>^3\Sigma_g^-</math>)</b>	-887.343545	999.9	2.0
<b>Ti<sub>2</sub>C(<math>^3B_2</math>)</b>	-1736.838854	231.9, 774.9, 802.4	2.001
<b>TiC<sub>2</sub>(<math>^3B_2</math>)</b>	-925.490288	576.5, 1060.9, 1646.9	2.0

units of the density matrix to obtain the charges on different centers. The Ti(0.679e)—C(-0.679e) bonds are slightly ionic due to the charge transfer from the metal to the carbon. The natural electronic configuration of Ti is  $4s^{0.91}3d^{2.38}4p^{0.06}$ , while that of C is  $2s^{1.31}2p^{3.32}3s^{0.02}$ .

The linear isomer with internal Ti atoms, (2,3) **II** lies well above **Iq** and the most stable isomer (**VIq**), due to the weaker Ti—Ti bond as compared to the C—C bond. The Ti—Ti, Ti—C,

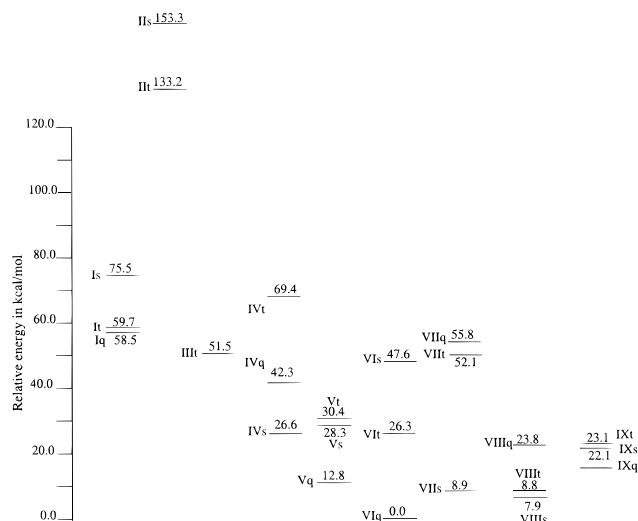


**Figure 3.** Plot of the relative energies (kcal/mol) of the various isomers in different electronic states of the  $\text{Ti}_2\text{C}_2$  cluster.

**TABLE 3: DFT Optimized Bond Lengths in Å of the Nonplanar Isomer IXs in Its Singlet State Using Different Functionals**

functionals	C–C	C–Ti	Ti–Ti
B3LYP	1.597	1.880	2.569
BVWN	1.624	1.905	2.614
SVWN	1.575	1.864	2.534
BP86	1.611	1.887	2.574
SVWN5	1.576	1.863	2.535
HF	1.251	2.331	2.861
B3LYP/3-21G	1.915	1.871	2.533
B3LYP/6-31G**	1.805	1.884	2.545

**TABLE 4: Calculated Binding Energies of the  $\text{Ti}_2\text{C}_2$  Cluster in kcal/mol**

product limits	binding energy
$2\text{Ti} + 2\text{C} \rightarrow \text{Ti}_2\text{C}_2$	328.78
$\text{Ti}_2 + \text{C}_2 \rightarrow \text{Ti}_2\text{C}_2$	232.43
$2\text{TiC} \rightarrow \text{Ti}_2\text{C}_2$	163.14
$\text{TiC}_2 + \text{C} \rightarrow \text{Ti}_2\text{C}_2$	65.97
$\text{Ti}_2\text{C} + \text{C} \rightarrow \text{Ti}_2\text{C}_2$	158.81

and C–C bond strengths in the diatomic molecule<sup>61</sup> are respectively  $33.8 \pm 5$ ,  $104 \pm 6$ , and  $145 \pm 5$  kcal/mol. Curiously, **III**t shows a significantly large Ti–Ti (3.101 Å) bond distance and can be visualized as the addition of two TiC molecules through the titanium atoms. The Ti–C distance in **II** is close to that of the isolated TiC molecule. The harmonic vibrational analysis of **II**s and **II**q reveals it to be a higher order saddle point, while the triplet state is characterized to be a minimum. However, it has four low magnitude vibrations (less than  $85 \text{ cm}^{-1}$ ), indicating a loose structure.

The other conceivable linear structures are those with the titanium atoms in the 1,2- and 1,3-positions. We have not attempted to optimize the latter two structures since our experience in  $\text{Ti}_2\text{C}$  and  $\text{TiC}_2$  suggests that linear isomers with alternating titanium and carbon atoms are unstable. We had problems of SCF convergence for the 1,2-isomer, and hence we are unsuccessful in optimizing this isomer in any of the electronic states.

**3.2. Three-Membered Ring Structures: III and IV.** Isomers **III** and **IV** can be viewed as the result of a 1-fold addition of a titanium or a carbon atom, respectively, to the predicted stable structure of  $\text{TiC}_2$ <sup>34</sup> and  $\text{Ti}_2\text{C}$ .<sup>62</sup> These isomers, respectively, with exocyclic Ti–Ti and C–C bonds have been identified as first-order saddle points from the diagonalization

of their Hessian matrix. Analysis of the eigenvectors corresponding to the negative eigenvalue of the force constant matrix suggests isomers **III** and **IV** to be transition structures for the degenerate rearrangement to **VIII**. A similar behavior has been observed for the analogous three-membered ring structures of  $\text{SiC}_3$ <sup>43</sup> and  $\text{Si}_2\text{C}_2$ <sup>44</sup> clusters. This observation in combination with our earlier observation<sup>35,36</sup> of unstable three-membered ring structures in  $\text{TiC}_3$  and  $\text{Ti}_2\text{C}_3$  systems implies that the 1-fold addition of either carbon or titanium leads to thermodynamically unfavorable products. The SCF convergence problems were encountered while optimizing the isomer **III** in its singlet and quintet states, and all our attempts to optimize its geometry on these two surfaces are proved futile. In spite of being saddle points, we have tabulated the harmonic frequencies and relative energies in Table 3 for the sake of completion. From Figure 3 it can be deduced that both these three-membered ring structures are energetically disposed above the most stable isomer, **VI**q.

**3.3. Four-Membered Ring Structures: V–VIII.** In searching for other low lying isomers of  $\text{Ti}_2\text{C}_2$ , one should expect that the presence of strong carbon–carbon bonds is favorable over the presence of weaker Ti–C and Ti–Ti bonds. Since inverted tricoordinated carbon and X (B, Be, Si, Ti) atoms are well documented<sup>35,43,44,63</sup> for rhombic  $\text{C}_3\text{Be}$ ,  $\text{C}_3\text{BH}$ ,  $\text{C}_3\text{Si}$ ,  $\text{C}_3\text{Ti}$ , and  $\text{C}_2\text{Si}_2$ , it is conceivable to have three four-membered cyclic structures, respectively, with two inverted carbon atoms (**VI**), with two inverted titanium atoms (**VII**), and with an inverted carbon and a titanium (**VIII**). Besides these nuclear arrangements, it is possible to envisage a trapezoidal structure **V** that could result from an in-plane 2 + 2 cycloaddition of  $\text{Ti}_2$  and  $\text{C}_2$  molecules. All these four probable cyclic planar structures have been considered for optimization in their lowest singlet, triplet, and quintet states.

**3.3.1. Rhombic Dicarbide: VI.** Of the three four-membered cyclic isomers, isomer **VI** with a transannular C–C bond is more stable compared to **VII** due to the obvious reason that the latter is stabilized only by a much weaker Ti–C bond. Structure **VIII** with a transannular Ti–C bond lies energetically between the other two rhombic isomers, viz., **VI** and **VII** (Figure 3). The transannular C–C bond distance in **VI**q (1.401 Å) is indicative of a significant C–C interaction, which is decreasing from quintet (1.401 Å) to triplet (1.516 Å) and singlet (1.518 Å). The transannular C–C bond distance in the similar rhombic isomers of  $\text{TiC}_3$ ,<sup>35</sup>  $\text{SiC}_3$ ,<sup>43</sup> and  $\text{Si}_2\text{C}_2$ <sup>44</sup> clusters are respectively 1.440, 1.441, and 1.425 Å. The vibrational analysis of **VI** characterizes it to be a minimum on the singlet, triplet, and quintet potential energy surfaces. The corresponding rhombic dicarbide isomer has also been calculated to be the global minimum on  $\text{Si}_2\text{C}_2$ <sup>44</sup> and  $\text{SiC}_3$ <sup>43</sup> potential energy surfaces. The attack of a titanium atom on the C–C bond of  $\text{TiC}_2$  leaves the multiply bonded carbons intact and thereby contributes to its stability. The Ti–C bond distances show appreciable variations ranging from 1.888 to 1.971 Å, and their Mulliken bond order varies from 1.40 to 1.14. The atomic charge on Ti and C as calculated by NBO analysis equals 0.695e and  $-0.695e$ , respectively. The natural electron configuration of C is calculated to be  $2s^{1.48}2p^{3.18}3s^{0.02}$  and that of Ti is  $4s^{0.82}3d^{2.47}4p^{0.02}$ . These findings imply a fairly high amount of ionic character present in the Ti–C bonds, a conclusion that has been seen to be true for all the isomers.

The nature of the bonding in this isomer can be understood from the analysis of the CASSCF molecular orbitals. The electronic configuration of the singlet state corresponds to  $9a_g^2 4b_{3u}^2 6b_{2u}^2 3b_{1g}^2 3b_{1u}^2 1b_{2g}^2 2b_{3g}^2$  with a core electron configuration of  $6a_g^2 3b_{3u}^2 5b_{2u}^2 2b_{1g}^2 2b_{1u}^2 2b_{2g}^2$ . The valence orbitals of **VI** and **VII**

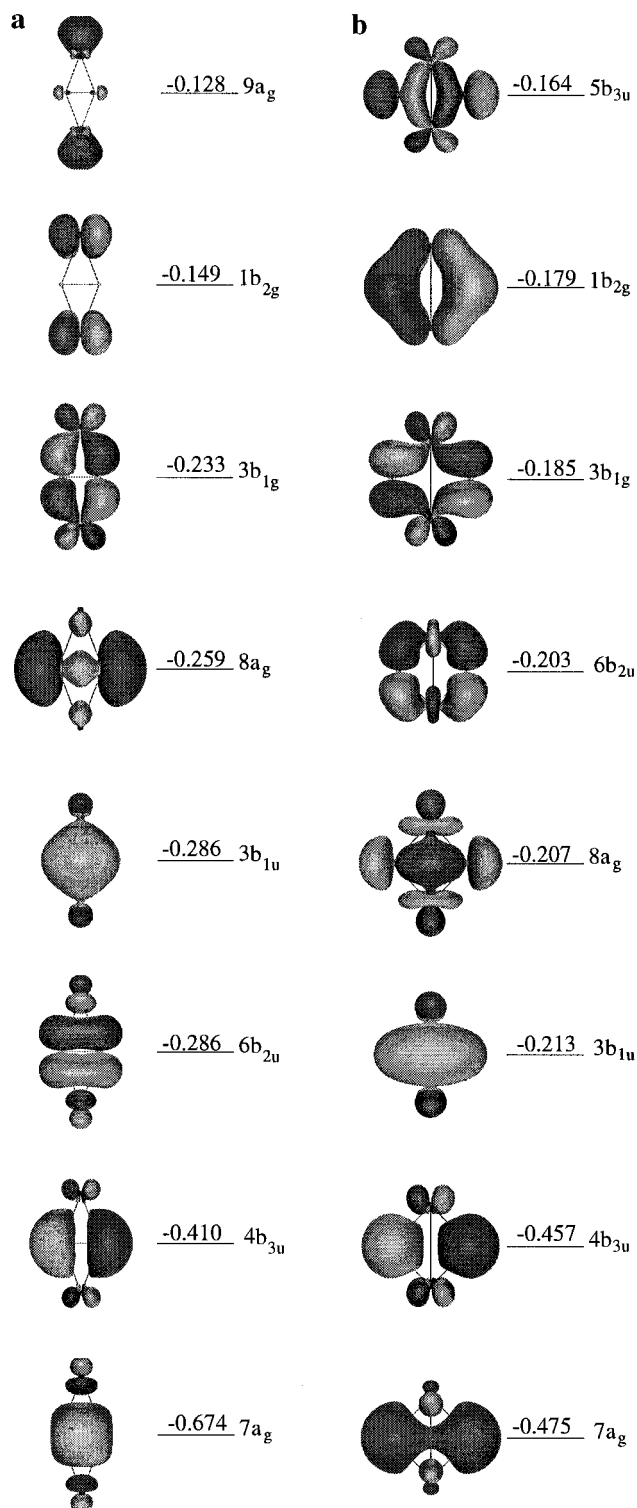


**Figure 4.** Highest occupied MO's for (a) rhombic dicarbide and (b) rhombic dititanide isomers of  $\text{Ti}_2\text{C}_2$ .

are shown in Figure 4. The carbon atoms are placed on the  $x$ -axis, while the titanium atoms are on the  $y$ -axis. The  $7a_g$  orbital undoubtedly portrays the C–C  $\sigma$  bond character. It is appropriate to mention that in  $\text{C}_4$ <sup>63</sup> and  $\text{Si}_2\text{C}_2$ <sup>44</sup> such a  $\sigma$  bond has not been observed. Lammertsma reported a nonbonding or  $\sigma$ -bond-deficient character between the transannular nearby carbons of  $\text{C}_4$  (HOMO orbital 12,  $a_g$  in ref 63) and the electron density was mainly located outside the molecule. A similar  $\sigma$ -deficient bonding has been observed for  $\text{Si}_2\text{C}_2$  (HOMO orbital 20,  $a_g$  in ref 44) too.

The  $8a_g$  and  $4b_{3u}$  orbitals depict the symmetry-adapted combinations of the carbon lone pairs. While the  $6b_{2u}$  orbital corresponds to the in-plane  $\pi$  bond between the carbons, the  $3b_{1u}$  corresponds to the  $\pi_{\perp}$  orbital of the  $\text{C}_2$  moiety. As can be seen from Figure 4, the  $3b_{1u}$  orbital is delocalized over all four atoms, and the metal atoms exert a bonding interaction with the carbon  $\pi$  cloud via the  $d_{yz}$  orbitals. With respect to metals, the  $3b_{1u}$  orbitals represents a  $\pi$  interaction. It is worthwhile to compare the corresponding orbitals of  $\text{C}_4$  and  $\text{Si}_2\text{C}_2$ . In  $\text{C}_4$ , the  $\pi_{\perp}$  orbital (MO 11,  $b_{3u}$  of ref 63) displays four-center (aromatic)  $\pi$  bonding and therefore the transannular carbons interaction was also found to be  $\pi$  bond deficient. However, in  $\text{Si}_2\text{C}_2$ , a direct  $\pi$  overlap (MO 17 of ref 44) has been reported, leading to enhanced C–C bonding in  $\text{Si}_2\text{C}_2$  owing to the larger polarizability of silicon. Thus, in contrast to the  $s^2p^2$  systems, the transannular carbons of  $\text{Ti}_2\text{C}_2$  are strongly bound via the C–C bonding orbitals  $7a_g$ ,  $6b_{2u}$ , and  $3b_{1u}$ .

In the doubly occupied  $3b_{1g}$  orbital, the  $\pi^*$  orbital of  $\text{C}_2$  exhibits a bonding interaction with the  $d_{xy}$  orbitals of metals. It could be viewed as a metal to ligand back-bonding ( $d$ – $p$  bonding) orbital. Since the  $\pi^*$  orbital of the  $\text{C}_2$  ligand is vacant, the  $3b_{1g}$  orbital in fact portrays the charge transfer from the metal to the ligand and is unique for the  $s^2d^2$  configuration. In the quintet state, the configuration of the unpaired electrons equals  $9a_g^1 7b_{2u}^1 1b_{2g}^1 1a_u^1$ . All these four orbitals have predominant metal lone pair character.

To summarize, the carbon atoms are  $sp$  hybridized and the  $\text{C}_2$  ligand orbitals in **VI** are  $7a_g$  ( $\sigma$ ),  $8a_g$  (lone pair),  $4b_{3u}$  (lone pair),  $6b_{2u}$  ( $\pi$ ),  $3b_{1u}$  ( $\pi_{\perp}$ ), and  $3b_{1g}$  ( $\pi^*$ ) and are doubly occupied. The fact that the lone pair orbitals of the isolated  $\text{C}_2$  are doubly occupied in  $\text{Ti}_2\text{C}_2$  suggests that it has acquired two electrons from the metal. The metal atoms exert bonding interactions with the ligand  $\pi$  ( $3b_{1u}$ ) and  $\pi^*$  ( $3b_{1g}$ ) orbitals, respectively, via the  $d_{yz}$  and  $d_{xy}$  orbitals.

**3.3.2. Rhombic Dititanide: VII.** The isomer **VII** with inverted titanium atoms is the predicted structure of  $\text{Ti}_2\text{C}_2$  by Reddy and Khanna.<sup>45</sup> Our calculations reveal it to be energetically  $\sim 8.97$  kcal/mol above the global minimum, **VIq**, and lies energetically above the isomer **VIII**. It is quite perceivable due to the existence of a C–C bond in isomer **VIII**. The peripheral Ti–C bond lengths vary from 1.837 to 1.898 Å in different electronic states. Thus, the peripheral Ti–C bonds are stronger than those of the rhombic dicarbide isomer (1.888–1.971 Å) (**VI**). The cross ring Ti–Ti distance is of the range 2.628–2.724 Å, and the Mulliken overlap population between the titanium atoms in the singlet state equals 1.154. This isomer has been identified as a minimum on its singlet surface.

Analysis of the CASSCF molecular orbital framework gives a clear picture of the bonding properties in **VII**s than the bond distances. The ground singlet state configuration corresponds to  $8a_g^2 5b_{3u}^2 6b_{2u}^2 3b_{1g}^2 3b_{1u}^2 1b_{2g}^2 2b_{3g}^2$  with the same core electron configuration as in isomer **VI**. The carbon atoms remain unhybridized. The valence  $7a_g$  orbital corresponds to the carbon  $2s$  orbitals, and it has a very minor contribution from titanium atoms. The  $8a_g$  orbital shows a Ti–Ti  $\sigma$  bond, but it has an appreciable overlap with the carbon  $p$  orbitals. This orbital suggests the concentration of the electron density in the center of the ring rather than in the periphery. The  $4b_{3u}$  orbital is a lone pair orbital on carbon and corresponds to the symmetry counterpart of  $7a_g$ . The  $5b_{3u}$  orbital depicts a Ti–Ti  $\pi$  bond formed via the  $d_{xy}$  orbitals of titaniums with a strong  $\sigma$  bonding interaction with the  $p_x$  orbitals of the carbon atoms. It represents a four-center two-electron ( $4c-2e$ ) orbital wherein the two carbons are bonded to the  $\pi$  cloud of the  $\text{Ti}_2$  moiety. The  $6b_{2u}$

orbital has predominantly a carbon character but with a strong bonding interaction with the  $d_{x^2}$  orbital of titanium. The  $3b_{1g}$  orbital is the symmetry counterpart of  $6b_{2u}$ . Though the  $p_y$  orbitals of the carbon are in an opposite phase, they are exerting a strong bonding interaction with the symmetry appropriate  $d_{xy}$  orbital of Ti. With respect to the metal part, the  $3b_{1g}$  orbital is a  $\pi^*$  orbital and between Ti and C it corresponds to a  $\sigma$  bonding. In the  $3b_{1u}$  orbital, the  $p_z$  orbitals of the carbon atoms interact with the  $\pi_{\perp}$  of the  $Ti_2$  moiety, and thereby it gives rise to a  $4c-2e$   $\pi$  orbital. The  $1b_{2g}$  orbital is a very covalent bond between Ti and C. With respect to  $Ti_2$  it corresponds to a  $\delta$  interaction via the  $d_{xz}$  orbitals of titanium, and between Ti and C it corresponds to a  $\pi$  overlap.

On the whole, we could identify  $\sigma$  ( $8a_g$ ),  $\pi$  ( $5b_{3u}$ ),  $\pi_{\perp}$  ( $3b_{1u}$ ), and  $\delta$  ( $1b_{2g}$ ) bonds in the  $Ti_2$  moiety. The strong interaction between the metal and the carbon qualitatively suggests the covalent nature of the isomer **VII** as in the bulk fcc TiC and explains the multiple bonding between Ti and C. Owing to the strong interaction between the metal and the carbon orbitals, we expect isomer **VII** to be more covalent than **VI**.

**3.3.3. Rhomboidal  $Ti_2C_2$ : VIII.** Optimization of the rhombic structure with both an inverted carbon and a titanium leads to rhomboidal geometry with a transannular Ti–C bond. This isomer may be viewed as a side on complex of Ti to one of the Ti–C bonds of  $TiC_2$  (Scheme 1). This isomer is found to be a minimum in all three investigated states of different multiplicities, and the energy difference between the singlet and triplet states is very small. The transannular Ti–C distance in the triplet state is 2.116 Å and is therefore suggestive of significant Ti–C bonding across the ring. The Mulliken bond order for the peripheral Ti–C bonds in **VIII**t are 1.39 and 1.18, while the transannular Ti–C bond order is 0.63. Corresponding rhomboidal structure with inverted silicon and carbon has been predicted to be the second best structure in the case of the group IVA clusters,  $C_2Si_2$  and  $SiC_3$ . The natural population analysis yields a charge distribution as follows; 0.676e and 0.449e on titaniums and  $-0.439e$  and  $-0.686e$  on carbons.

**3.4. Nonplanar Structure: IX.** In addition to these planar four-membered ring structures, we also have investigated a nonplanar structure **IX** with maximum bond valencies on carbon and titanium atoms. Optimization leads to a stable minimum on singlet and quintet states and is energetically more stable in its quintet state (see Figure 3). The C–C bond distance of 1.309 and 1.310 Å in the triplet and quintet states suggests a multiply bonded  $C_2$  moiety. The calculated Mulliken bond orders in the triplet and quintet states are respectively 1.72 and 1.73. However, on the singlet surface the C–C bond has been elongated (1.589 Å with a bond order of 0.73) with a consequent shortening and strengthening of the Ti–C bonds (1.880 Å with a bond order of 1.40). The Ti–Ti bond distance of 2.323 Å in the triplet state suggests multiply bonded titaniums. Such a nonplanar structure has not been obtained for  $Si_2C_2$  and  $SiC_3$  and it has been identified as a transition structure in the case of the isovalent electronic  $TiC_3$ . The existence of such a nonplanar structure is related to the floppiness of the rhomboidal structure to significant nonplanarity. However, it is often sensitive to (i) the size of the basis set, (ii) the extent of incorporation of the effects of electron correlation, and (iii) the multireference character. In order to derive an understanding about its dependence on the size of the basis set, we performed two calculations with smaller basis sets, namely, 3-21G and 6-31G\*\*. It is apparent from Table 3, that the stability of this isomer depends heavily on the size of the basis set. With smaller basis sets we do get a nonplanar minimum, however, without a

carbon–carbon bonding. We have also performed DFT calculations with various functionals using the larger basis set. We found larger variations in the geometry with various functionals (Table 3), the C–C bond length varies from 1.575 to 1.624 Å, and the C–Ti bond length varies from 1.863 to 1.905 Å. Also, the spin contamination for the triplet and quintet state geometries (refer Table 2) are appreciable and it thereby obfuscates the conclusion regarding its relative stability. Furthermore, numerically estimated second derivative matrices using the MUL-LIKEN program suggest it to be a minimum on all three surfaces. However, the analytical derivatives (Table 2) have two imaginary frequencies for the triplet multiplicity. All these calculations demonstrate the sensitivity of this nonplanar minimum to the level of characterization and it demands a multireference study with an extended basis set. Unfortunately, for the time being an appropriate multireference study (CAS-(16,20)) is beyond our computational resources. In view of its unique nature, this nonplanar structure in other tetraatomic clusters deserves a further study by its own. However, the CAS-(6,12) calculation has revealed that it involves the contribution (squared weight  $|c_i^2|$ ) of the ground state configuration amounting to 0.717. Hence, extensive multireference calculations are needed to fully characterize this isomer and to establish its relative stability.

**3.5. Trapezoidal Titanium Dicarbide: V.** Trapezoidal orientation of the four atoms leads to a second-order saddle point geometry in singlet, triplet, and quintet state PESs. The geometrical parameters are presented here for the sake of comparison, and we will not discuss its bonding characteristics. Singlet trapezoid **Vs** with triply bonded carbons (1.286 Å) has two imaginary frequencies, viz.,  $464.7i$   $cm^{-1}$  of the  $b_2$  symmetry, indicating an in-plane deformation to the rhomboidal structure **VIIIs**, and  $160.6i$   $cm^{-1}$  of the  $a_2$  frequency, suggesting a distortion to nonplanarity. The triplet trapezoid **Vt** also has similar normal modes with imaginary frequencies. The imaginary  $b_2$  frequency of  $488.i$   $cm^{-1}$  indicates an in-plane deformation. As can be seen from Figure 2, the C–C and C–Ti bond distances are very much the same in all three electronic states. However, the Ti–Ti distance shows appreciable deviations (2.114–2.868 Å) with the spin multiplicity of the state.

The binding energy of the cluster with respect to different atomic and molecular limits are tabulated in Table 4. The cluster is stabilized by 14.26 eV with respect to the atomic carbon and titanium. The cluster could easily dissociate into  $TiC_2 + Ti$ , and this, in turn, provides a clue that  $TiC_2$  could be the growth species in the  $Ti_8C_{12}$  cluster formation. As is obvious from Figure 3, several isomers exist as a minimum within 70 kcal/mol of energy from the global minimum and in plasma temperature the relative population of all these higher energy isomers would be appreciable and hence there exists a certain probability for them to play a role in the metcar formation.

## 4. Conclusions

The results of our calculations predict a rhombic dicarbide structure **VI** for the ground state molecular structure of  $Ti_2C_2$ . Various other ring structures **VII–VIII** also correspond to a minima, however, with higher energies. Besides these planar ring structures, calculations also suggest a nonplanar minimum **IX** for  $Ti_2C_2$ . Ring structures with exocyclic double bonds (**III** and **IV**) are identified as transition structures with respect to the degenerate rearrangement to the rhomboidal structure. The comparison of the preferred geometries of  $Ti_nC_m$  clusters ( $n = 1, 2, m = 2, 3, 4$ ) with the analogous group IVA silicon–carbon clusters follows:  $SiC_2$  (cyclic,  $C_{2v}$ ) is similar to  $TiC_2$ ;  $SiC_3$  is

rhomboidal as TiC<sub>3</sub> but with a transannular C–C bond instead of a Si–C bond; Si<sub>2</sub>C<sub>2</sub> is a rhombic dicarbide as Ti<sub>2</sub>C<sub>2</sub> (however, in Si<sub>2</sub>C<sub>2</sub> the nonplanar isomer is a saddle point); SiC<sub>4</sub> and Si<sub>2</sub>C<sub>3</sub> are linear, contrary to TiC<sub>4</sub> and Ti<sub>2</sub>C<sub>3</sub>, which are cyclic. The Ti–C bonds are highly ionic and the main energetic difference between the various isomers comes from the delocalization of the transferred charge from titanium to carbon. The calculated ground-state geometries and frequencies will be valuable for identifying these clusters experimentally and in turn for testing the validity of the DFT predictions. Clearly, theoretical calculations on additional Ti<sub>n</sub>C<sub>m</sub> clusters are needed to elucidate the intermediates involved in the cluster formation, to identify the growth species, and to investigate the clustering phenomenon.

**Acknowledgment.** We are indebted to the Fund for Scientific Research (FWO-Vlaanderen) and Geconceerteerde Onderzoeksakties (GOA) for financial support and to the KU Leuven Computer center for providing computer facilities.

## References and Notes

- (1) Guo, B. C.; Kerns, K. P.; Castleman, A. W., Jr. *Science* **1992**, *255*, 1411.
- (2) Guo, B. C.; Wei, S.; Purnell, J.; Buzza, S. A.; Castleman, A. W., Jr. *Science* **1992**, *256*, 515.
- (3) (a) Wei, S.; Guo, B. C.; Purnell, J.; Buzza, S.; Castleman, A. W., Jr. *Science* **1992**, *256*, 818. (b) Wei, S.; Castleman, A. W., Jr. *Chem. Phys. Lett.* **1994**, *227*, 305.
- (4) (a) Wei, S.; Guo, B. C.; Purnell, J.; Buzza, S.; Castleman, A. W., Jr. *J. Phys. Chem.* **1992**, *96*, 4166. (b) May, B. D.; Cartier, S. F.; Castleman, A. W., Jr. *Chem. Phys. Lett.* **1995**, *242*, 265.
- (5) Guo, B. C.; Kerns, K. P.; Castleman, A. W., Jr. *J. Am. Chem. Soc.* **1993**, *115*, 7415.
- (6) Guo, B. C.; Wei, S.; Chen, Z.; Kerns, K. P.; Purnell, J.; Buzza, S.; Castleman, A. W., Jr. *J. Chem. Phys.* **1992**, *97*, 5243.
- (7) Chen, Z. Y.; Guo, B. C.; May, B. D.; Cartier, S. F.; Castleman, A. W., Jr. *Chem. Phys. Lett.* **1992**, *198*, 118.
- (8) Wei, S.; Guo, B. C.; Purnell, J.; Buzza, S. A.; Castleman, A. W., Jr. *J. Phys. Chem.* **1993**, *97*, 9559.
- (9) Kerns, K. P.; Guo, B. C.; Deng, H. T.; Castleman, A. W., Jr. *J. Chem. Phys.* **1994**, *101*, 8529.
- (10) Cartier, S. F.; Chen, Z. Y.; Walder, G. J.; Sleppy, C. R.; Castleman, A. W., Jr. *Science* **1993**, *260*, 195.
- (11) Cartier, S. F.; May, B. D.; Toleno, B. J.; Purnell, J.; Wei, S.; Castleman, A. W., Jr. *Chem. Phys. Lett.* **1994**, *220*, 23.
- (12) Wei, S.; Guo, B. C.; Deng, H. T.; Kerns, K. P.; Purnell, J.; Buzza, S. A.; Castleman, A. W., Jr. *J. Am. Chem. Soc.* **1994**, *116*, 4475.
- (13) (a) Cartier, S. F.; May, B. D.; Castleman, A. W., Jr. *J. Chem. Phys.* **1994**, *100*, 5384. (b) Cartier, S. F.; May, B. D.; Castleman, A. W., Jr. *J. Am. Chem. Soc.* **1994**, *116*, 5295. (c) Deng, H. T.; Guo, B. C.; Kerns, K. P.; Castleman, A. W., Jr. *Int. J. Mass Spectrom. Ion Processes* **1994**, *138*, 275.
- (14) Guo, B. C.; Castleman, A. W., Jr. In *Advances in Metal and Semiconductor Clusters*; Duncan, M. A., Ed.; JAI Press: Greenwich, CT, 1994; Vol. II.
- (15) Pilgrim, J. S.; Duncan, M. A. *J. Am. Chem. Soc.* **1993**, *115*, 6958.
- (16) (a) Bowers, M. T. *Acc. Chem. Res.* **1994**, *27*, 324. (b) von Helden, G.; Gotts, N. G.; Maitre, P.; Bowers, M. T. *Chem. Phys. Lett.* **1994**, *227*, 601. (c) Lee, S.; Gotts, N. G.; von Helden, G.; Bowers, M. T. *Science* **1995**, *267*, 999.
- (17) Pauling, L. *Proc. Natl. Acad. Sci. U.S.A.* **1992**, *89*, 8175.
- (18) (a) Lin, Z.; Hall, M. B. *J. Am. Chem. Soc.* **1992**, *114*, 10054. (b) Lin, Z.; Hall, M. B. *J. Am. Chem. Soc.* **1993**, *115*, 11165.
- (19) (a) Rohmer, M. M.; de Vaal, P.; Benard, M. *J. Am. Chem. Soc.* **1992**, *114*, 9696. (b) Rohmer, M. M.; Henriot, C.; Bo, C.; Poblet, J. P. *J. Chem. Soc., Chem. Commun.* **1993**, 1182. (c) Rohmer, M. M.; Benard, M.; Bo, C.; Poblet, J. M. *J. Am. Chem. Soc.* **1995**, *117*, 508.
- (20) Reddy, B. V.; Khanna, S. N.; Jena, P. *Science* **1992**, *258*, 1640.
- (21) Hay, P. J. *J. Phys. Chem.* **1993**, *97*, 3081.
- (22) Reddy, B. V.; Khanna, S. N. *Chem. Phys. Lett.* **1993**, *209*, 104.
- (23) Chen, H.; Feyereisen, M.; Long, X. P.; Fitzgerald, G. *Phys. Rev. Lett.* **1993**, *71*, 1732.
- (24) Grimmes, R. W.; Gale, J. D. *J. Phys. Chem.* **1993**, *97*, 4616.
- (25) Lou, L.; Guo, T.; Norlander, P.; Smalley, R. E. *J. Chem. Phys.* **1993**, *99*, 5301.
- (26) Khan, A. *J. Phys. Chem.* **1993**, *97*, 10937.
- (27) (a) Dance, I. G. *J. Chem. Soc., Chem. Commun.* **1992**, 1779. (b) Dance, I. G. *J. Chem. Soc., Chem. Commun.* **1993**, 1306. (c) Dance, I. G. *J. Am. Chem. Soc.* **1993**, *115*, 11052.
- (28) Lou, L.; Nordlander, P. *Chem. Phys. Lett.* **1994**, *224*, 439.
- (29) Reddy, B. V.; Khanna, S. N. *J. Phys. Chem.* **1994**, *98*, 9446.
- (30) Li, Z.; Gu, B.; Han, R.; Zheng, Q. *Z. Phys. D* **1993**, *27*, 275.
- (31) Rohmer, M. M.; Benard, M.; Bo, C.; Poblet, J. M. *J. Am. Chem. Soc.* **1995**, *117*, 508.
- (32) Yeh, C. S.; Afzaal, S.; Lee, S. A.; Byun, Y.; Freiser, B. S. *J. Am. Chem. Soc.* **1994**, *116*, 8806.
- (33) Li, S.; Wu, H.; Wang, L.-S. *J. Am. Chem. Soc.* **1997**, *119*, 7417.
- (34) Sumathi, R.; Hendrickx, M. *Chem. Phys. Lett.* **1998**, *287*, 496.
- (35) Sumathi, R.; Hendrickx, M. *J. Phys. Chem.* **1998**, *102*, 496.
- (36) Sumathi, R.; Hendrickx, M. *J. Phys. Chem.* **1998**, *102*, 7308.
- (37) (a) Lammertsma, K.; Güner, O. F.; Sudhakar, P. V. *J. Chem. Phys.* **1991**, *94*, 8105. (b) Lammertsma, K.; Pople, J. A.; Schleyer, P. v. R. *J. Am. Chem. Soc.* **1986**, *108*, 7. (c) Ritchie, J. P.; King, H. F.; Young, W. S. *J. Chem. Phys.* **1986**, *85*, 5175. (d) Magers, D. H.; Harrison, R. J.; Bartlett, R. J. *J. Chem. Phys.* **1986**, *84*, 3284. (e) Rao, B. K.; Khanna, S. N.; Jena, P. *Solid State Commun.* **1986**, *58*, 53. (f) Whiteside, R. A.; Krishnan, R.; DeFrees, D. J.; Pople, J. A.; Schleyer, P. v. R. *Chem. Phys. Lett.* **1981**, *78*, 538.
- (38) (a) Shen, L. N.; Graham, W. R. M. *J. Chem. Phys.* **1989**, *91*, 5115. (b) Health, J. R.; Saykally, R. J. *J. Chem. Phys.* **1991**, *94*, 3271. (c) Kranze, R. H.; Graham, W. R. M. *J. Chem. Phys.* **1991**, *96*, 2517.
- (39) (a) Zajfman, D.; Feldman, H.; Heber, O.; Kella, D.; Majer, D.; Vager, Z.; Nalaman, R. *Science* **1992**, *258*, 1129. (b) Kella, D.; Zajfman, D.; Heber, O.; Majer, D.; Feldman, H.; Vager, Z.; Nalaman, R. *Z. Phys. D* **1993**, *26*, 340.
- (40) Arnold, D. W.; Bradforth, S. E.; Kitsopoulos, T. N.; Neumark, D. M. *J. Chem. Phys.* **1991**, *95*, 8753.
- (41) (a) Martin, J. M. L.; Francois, J. P.; Gijbels, R. *J. Chem. Phys.* **1990**, *93*, 8850. (b) Martin, J. M. L.; Francois, J. P.; Gijbels, R. *J. Chem. Phys.* **1991**, *94*, 3753. (c) Martin, J. M. L.; Schwenke, D. W.; Lee, T. J.; Taylor, P. R. *J. Chem. Phys.* **1996**, *104*, 4657.
- (42) (a) Raghavachari, K. *J. Chem. Phys.* **1986**, *84*, 5672. (b) Raghavachari, K.; Logovinsky, V. *Phys. Rev. Lett.* **1985**, *55*, 2853.
- (43) Alberts, I. L.; Grev, R. S.; Schaefer, H. F., III. *J. Chem. Phys.* **1990**, *93*, 5046.
- (44) (a) Lammertsma, K.; Güner, O. F. *J. Am. Chem. Soc.* **1988**, *110*, 5239. (b) Sudhakar, P. V.; Güner, O. F.; Lammertsma, K. *J. Phys. Chem.* **1989**, *93*, 7289.
- (45) Reddy, B. V.; Khanna, S. N. *J. Phys. Chem.* **1994**, *98*, 9446.
- (46) Becke, A. D. *J. Chem. Phys.* **1993**, *98*, 5648.
- (47) Lee, C.; Yang, W.; Parr, R. G. *Phys. Rev. B* **1988**, *37*, 785.
- (48) Rice, J. E.; Horn, H.; Lengsfelds, B. H.; McLean, A. D.; Carter, J. T.; Replogle, E. S.; Barnes, L. A.; Maluender, S. A.; Lie, G. C.; Gutwiski, M.; Rude, W. E.; Sauer, S. P. A.; Lindh, R.; Anderson, K.; Chevalier, T. S.; Widmark, P.-O.; Bouzida, D.; Pacansky, G.; Singh, K.; Gillan, C. J.; Carnevali, P.; Swope, W. C.; Liu, B. *Mulliken Version 2.25b, internal release*; IBM Corp.: Almaden, CA, 1995.
- (49) Frisch, M. J.; Trucks, G. W.; Head-Gordon, M.; Gill, P. M. W.; Wong, M. W.; Foresman, J. B.; Johnson, B. G.; Schlegel, H. B.; Robb, M. A.; Replogle, E. S.; Gomperts, R.; Andres, J. L.; Raghavachari, K.; Binkley, J. S.; Gonzalez, C.; Martin, R. J.; Fox, D. J.; Defrees, D. J.; Baker, J.; Stewart, J. J. P.; Pople, J. A. *Gaussian 94*; Gaussian Inc.: Pittsburgh, PA, 1994.
- (50) TURBOMOLE, Version 2.3.5.; Biosym Technologies Inc.: San Diego, 1994.
- (51) Hertwig, R. H.; Koch, W. *Chem. Phys. Lett.* **1997**, *268*, 1997.
- (52) Vosko, S. H.; Wilk, L.; Nusair, M. *Can. J. Phys.* **1980**, *58*, 1200.
- (53) Perdew, J. P.; Wang, Y. *Phys. Rev. B* **1992**, *45*, 13244.
- (54) Wachters, A. J. H. *J. Chem. Phys.* **1970**, *52*, 1033. Wachters, A. J. H. *IBM Tech. Rep. RJ584*, **1969**.
- (55) Hay, P. J. *J. Chem. Phys.* **1977**, *66*, 4377.
- (56) Bauschlicher, C. W., Jr.; Langhoff, S. R.; Barnes, L. A. *J. Chem. Phys.* **1989**, *91*, 2399.
- (57) Stewart, R. F. *J. Chem. Phys.* **1970**, *52*, 431.
- (58) MOLPRO is a package of ab initio computer packages written by H.-J. Werner and P. J. Knowles with contributions from J. AlmÖf, R. D. Amos, S. Elbert, W. Meyer, E. A. Reinsch, R. Pitzer, and A. J. Stone.
- (59) (a) Hack, M. D.; Maclagan, R. G. A. R.; Scuseria, G. E.; Gordon, M. S. *J. Chem. Phys.* **1996**, *104*, 6628. (b) Bauschlicher, C. W.; Sigbahn, P. E. M. *Chem. Phys. Lett.* **1984**, *104*, 331.
- (60) Bernholdt, D. H.; Magers, D. H.; Bartlett, R. J. *J. Chem. Phys.* **1988**, *88*, 3612.
- (61) *CRC Handbook of Chemistry and Physics*, 63rd ed.; Weast, R. C., Ed.; CRC Press: Boca Raton, FL, 1983.
- (62) Sumathi, R.; Hendrickx, M. Unpublished results.
- (63) Lammertsma, K. *J. Am. Chem. Soc.* **1986**, *108*, 5127.